Nat. Hazards Earth Syst. Sci., 10, 1523–1530, 2010
www.nat-hazards-earth-syst-sci.net/10/1523/2010/
doi:10.5194/nhess-10-1523-2010

Natural Hazards and Earth System Sciences

Tight coupling UFMArcGIS for simulating inundation depth in densely area

S. H. Kang

Dept. of Civil Engineering, Kangwon National University, Samcheok, Republic of Korea

Received: 18 September 2008 – Revised: 11 June 2010 – Accepted: 29 June 2010 – Published: 14 July 2010

Abstract. The integration of hydrological models and Geographical Information Systems (GIS) usually takes two approaches: loose coupling and tight coupling. This paper presents a tight coupling approach within a GIS environment that is achieved by integrating the urban flood model with the macro language of GIS. Such an approach affords an uncomplicated way to capitalize on the GIS visualization and spatial analysis functions, thereby significantly supporting the dynamic simulation process of hydrological modeling. The tight coupling approach is illustrated by UFMArcGIS (Urban Flood Model with ArcGIS), which is a realization of an urban flood model integrated with the VBA (visual basic of application) language of ArcGIS. Within this model, major stages of model structures are created from the initial parameter input and transformation of datasets, intermediate maps are then visualized, and the results are finally presented in various graphical formats in their geographic context. This approach provides a convenient and single environment in which users can visually interact with the model, e.g. by adjusting parameters while simultaneously observing the corresponding results. This significantly facilitates users in the exploratory data analysis and decision-making stages in terms of the model applications.

1 Introduction

In recent years, the introduction of various hydraulic and hydrological modeling techniques has enabled users of GIS to go beyond the data inventory and management stage to conduct sophisticated modeling and simulation. In terms of hydrological modeling, GIS has provided modelers with new platforms for data management and visualization, particularly through its powerful capabilities to process topographical data. The rapid distribution of GIS techniques to a wider population has the potential to make various hydrological models more transparent and to enable the communication of GIS operations and results to a large group of users. Attempts have been made to integrate various models into GIS in order to meet the increasing need to enhance its functionality in environmental modeling (Bishop and Karadaglis, 1996; Vivoni et al., 2005), urban modeling (Nie, 2004; Hosoyamada, 2005; Takayama et al., 2006) and, in a more general sense, analytical tools (Horritt and Bates, 2001a, b; Yang and Rystedt, 2002; Haile and Rientjes, 2005; Sayama et al., 2006).

Consequently, while able to simplify reality, models can still involve complex mathematical and analytical exercises. While some of these calculations are possible within a GIS, others require greater computational abilities than are currently available in a GIS. Models can be implemented within a GIS in a number of ways (Sui and Maggio, 1999). The model and the GIS can be loosely coupled, whereby the GIS is used to prepare data for use in a separate computational model. The GIS can alternatively be used simply to visualize the model output. The model can also be implemented using the functionality of the GIS, for example in calculating topographic factors for a hydrological model. The advantages of this latter approach lie in the fact that both systems can either be developed or used independently. However, the exchange of data files, which usually involves taking text files as a link between two systems, is inherently cumbersome and not user-friendly. Alternatively, the model and the GIS can be tightly computationally coupled, whereby the GIS is used for both the input and the visualization of the output. It should be noted that differences in data models have a significant impact on the computational manipulation of data in the above coupling process. Compared with the loose coupling

Correspondence to: S. H. Kang
(kang7231@hanmail.net)

method used in the earlier development of GIS, tight coupling is considered to be a more effective integration method when a transparent interface is required for the data structures of GIS, which is rarely provided by GIS developers.

Previously employed for mapping analysis results, visualization is nowadays considered an important tool for spatial analysis (Bourget, 2004). Various new terms have been used to reflect this change, such as spatial data exploration and exploratory visualization. When hydraulic models are fully integrated into GIS, the analytical processes can be simulated, thereby making visual exploration more straightforward. With such a highly interactive platform, users are able to obtain a comprehensive perception of reality through its counterpart in computer systems. Despite these conveniences, few attempts have been made to tightly link a GIS based model to simulate inundation depth. This is due to the complex topographic features in urban areas.

In this study, an urban flood model – overland flow, urban flood flow and sewer flow – was combined and developed with ArcGIS in order to simulate inundation depth in Samcheok city, South Korea. The intention is to provide an example to illustrate the advantages of using such a tight integration method for modeling and visualization.

2 Description of study site

The Oship River of Samcheok city, Kangwon Province, in the Republic of Korea is located about 100 km to the east of Seoul ($128°30' \sim 128°40'$ E; $37°25' \sim 37°49'$ N). The drainage area of the Oship River basin is 384 km^2, with a mean annual precipitation of 1550 mm over the last 10 years (1998–2007; data are only available for this period). Over 80% of the annual mean rainfall area was concentrated in heavy showers that occurred several times during the rainy season from May to September during this period (WAMIS, 2009; on-line available at http://www.wamis.go.kr/).

The basin has a large forested area (87%) and an area for agricultural use (7.5%). The main channel length of the Oship River is 59 km and the channel slope ranges from 0.037 to 0.801%. Samcheok city is situated in the downland area of the Oship River basin, with a population of approximately 30 000 inhabitants. The total area of the city is 2.79 km^2 with contours ranging from 0 to 30 m for an urban flood simulation of 1.32 km^2. The area has a well known history of floods due to heavy rainfall (Kang, 2007). From 31 August to 1 September 2002, the basin endured a large flood due to heavy rainfall caused by Typhoon Rusa. The typhoon claimed the lives of 13 people and inundated 3639 houses and 200 ha of farmland. The maximum hourly and total precipitation was 64 mm h^{-1} and 582 mm, respectively. This devastation extended further when another typhoon hit the same region in 2003, resulting in serious damage. The successive disasters isolated the public, separating people from other towns, and paralyzed personal infrastructures, while causing wide-spread destruction of property and numerous human casualties. In order to reduce the loss of life and property caused by floods, the Flood Mitigation Project was initiated by the municipality of Samcheok city in 2004. The project was designed to protect against the 100-year flood frequency. The major components for reducing flood damage in the urban area include: drainage pumping stations, a sewer drainage system, and channel improvement. Other cities in the world have been developed similar projects. For example in Barcelona city (Spain) the damages produced by flash floods have considerably diminished during the last years basically due to the development of a dense network of pumping station within the city (Barrera et al., 2006).

3 Model structure

The overall model structure with ArcGIS is represented as shown in Fig. 1. Following the transformation of rainfall to effective runoff by interception and depression storage simulation, surface runoff is handled in two parallel simulation modules. The sub-routine module for hydrologic surface runoff is applied to areas where there is surface flooding as well as interaction between surface flow and sewer flow. Here, surface runoff enters the sewer system at defined inlets.

3.1 Overland flow from watershed

The drainage area of Oship River basin is 393 km^2 and has many tributaries. Among them, the study area for the surface runoff is 344.8 km^2 and the channel slope ranges from 0.071 to 0.40. The governing equations based on the kinematic wave model are as follows:

3.1.1 Slope flow

$$\frac{\partial h}{\partial t} + \frac{\partial q}{\partial x} = r_\mathrm{e} \tag{1}$$

$$q = \alpha h^m \tag{2}$$

Here, x is a one-dimensional spatial coordinate; t is time; q is the discharge per unit width on the slope; r_e is the effective rainfall; h is the water depth; α and m are constants, respectively (m'=5/3; $\alpha = \sqrt{\sin\theta}/N$; θ is the slope gradient; and N is the Manning's roughness coefficient in the slope).

3.1.2 River flow

$$\frac{\partial h}{\partial t} + \frac{\partial q'}{\partial x} = \frac{q}{B} \tag{3}$$

$$q' = \alpha h^{m'} \tag{4}$$

Here, q' is the discharge per unit width on the mountainous river; q is the lateral inflow per unit width from the slope; B is the mountainous river width; α and m' are constants

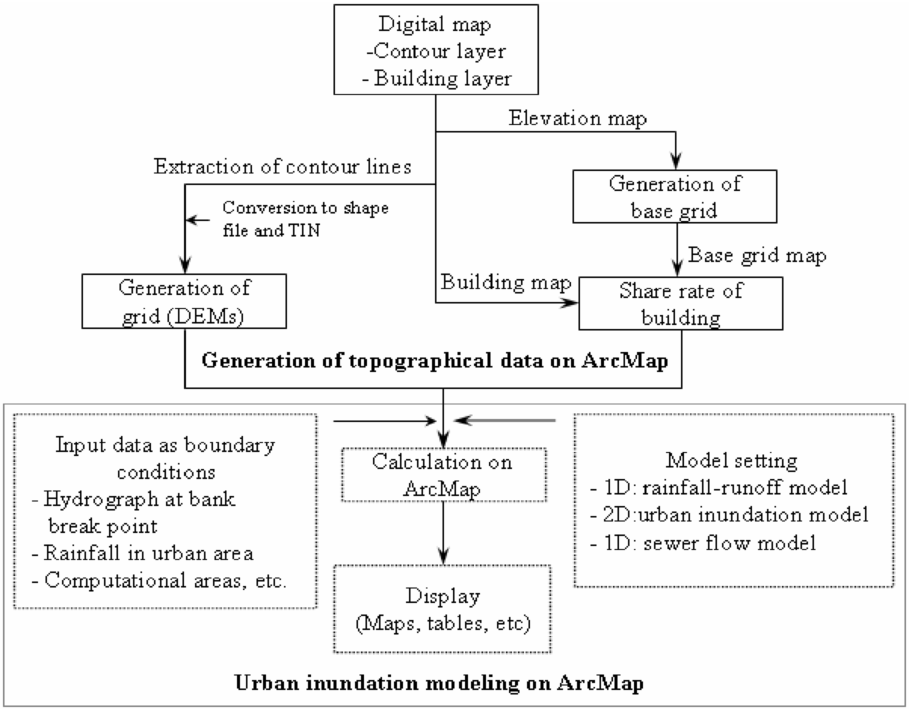

Fig. 1. Urban flood model structure on ArcGIS.

($\alpha = \sqrt{\sin\theta_r}/n$; θ_r is the river bed slope; n is the Manning's roughness coefficient; and m'=5/3).

The lateral inflow from the slope of the river is calculated using the characteristics method and the runoff discharge along the river is calculated using the finite difference method, which uses the Leap-Frog method. For the boundary condition in the down stream of the bank break point, the water-level flux of the sides of the grid is assigned using the discharge hydrograph as shown in Fig. 5.

3.1.3 Sewer flow

The rainwater in the sewer pipe is calculated in the following continuity and momentum equations:

$$\frac{\partial A}{\partial t} + \frac{\partial Q}{\partial x} = q \tag{5}$$

$$\frac{\partial Q}{\partial t} + \frac{\partial (uQ)}{\partial x} = gA\frac{\partial H}{\partial x} - \frac{gn^2|Q|Q}{R^{4/3}A}, \tag{6}$$

where A is the cross sectional area of flow; Q is the discharge; q is the lateral inflow; u is the flow velocity; H is the water level ($H = h + z$); and z is the elevation of the sewer pipe from the bottom (Abbott et al., 1998; Franz, 1997). For this study, the interaction between surface flow and sewer flow is as described by Schmitt et al. (2004). The value of Manning's roughness coefficient is $0.015\,\mathrm{s\,m^{-1/3}}$ and it is assumed that the cross sectional shape of the pipes is rectangular.

3.2 Urban flood flow

The governing equations for 2-D, gradually varied, unsteady flow can be derived from mass conservation and momentum equations. Overland flow equations are the 2-D expansion of St. Venant's 1-D open channel flow equations, as follows:

Continuity equation (mass conservation equation)

$$\frac{\partial h}{\partial t} + \frac{\partial M}{\partial x} + \frac{\partial M}{\partial y} = r_e - q_{out} + q_{over} \tag{7}$$

Momentum equations

$$\frac{\partial M}{\partial t} + \frac{\partial (uM)}{\partial x} + \frac{\partial (vM)}{\partial y} = -gh\frac{\partial H}{\partial x} - \frac{\tau_{bx}}{\rho_w} \tag{8}$$

$$\frac{\partial N}{\partial t} + \frac{\partial (uN)}{\partial x} + \frac{\partial (vN)}{\partial y} = -gh\frac{\partial H}{\partial y} - \frac{\tau_{by}}{\rho_w}, \tag{9}$$

where h is the water depth; u and v are the velocities of flow in the x- and y-directions, respectively; M and N are the fluxes of discharge in the x- and y-directions, respectively (M=uh, N=vh); q_{out} is the drainage discharge from the urban area to the sewer line in each grid; and q_{over} is the overtopping flow discharge per unit area of the computational grid from the down stream.

H is the water level, written as $H = h + z$, where z is the bed elevation. τ_{bx} and τ_{by} are the x- and y-components, respectively, of shear stress on the water bottom, as follows:

$$\tau_{bx} = \frac{\rho_w g n^2 u\sqrt{u^2+v^2}}{h^{1/3}} \tag{10}$$

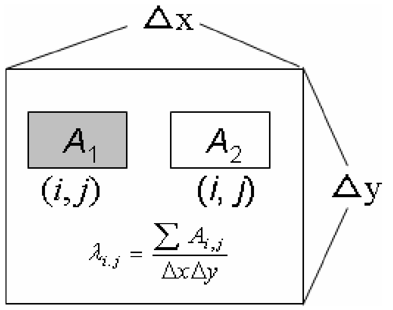

Fig. 2. Concept of buildings sharing (A_1) and (A_2) in each grid.

$$\tau_{\mathrm{by}} = \frac{\rho_{\mathrm{w}} g n^2 v \sqrt{u^2+v^2}}{h^{1/3}}, \tag{11}$$

where ρ_{w} is the water density; g is the gravity acceleration; and n is Manning's roughness coefficient.

4 Application of model

4.1 Influence of buildings

In order to simulate urban flooding, the influence of buildings should be carefully specified according to the needs of an application. GIS-based hydrological modeling is applied in order to distinguish the basic hydrological elements from a DEM (Digital Elevation Model). When considering the influence of buildings, the method of determining the share rate of a building is used as described in Eqs. (13) and (14). The possible representations of buildings for the model are illustrated in Fig. 2. In order to extract building properties, GIS techniques were applied as shown in Fig. 3. The data relating to building areas is converted into an image, which is then converted into a polygon using a geo-concept image. For extracting buildings, a minimum filter method by Arc-info was used.

In order to estimate the effect of a building, the share of the building $\lambda_{i,j}$ in each grid, and the transmissivity of the building $\beta_{i,j} = \sqrt{1-\lambda_{i,j}}$ are applied (Takahashi et al., 1986). In this study, buildings are represented as independently solid objects. For the calculation, the values of 1.0 for buildings and 0.0 for areas without buildings are assigned. The flux of discharge can then be defined as:

$$M^* = \beta M, \quad N^* = \beta N \tag{12}$$

where M^* and N^* are the flux of discharge which are corrected boundary conditions in the x- and y-components per unit width, respectively. If we consider M^*, N^* and λ, the continuity equation can be written as:

$$(1-\lambda)\frac{\partial h}{\partial t} + \frac{\partial M^*}{\partial x} + \frac{\partial N^*}{\partial y} = r_{\mathrm{e}} - q_{\mathrm{out}} + q_{\mathrm{over}} \tag{13}$$

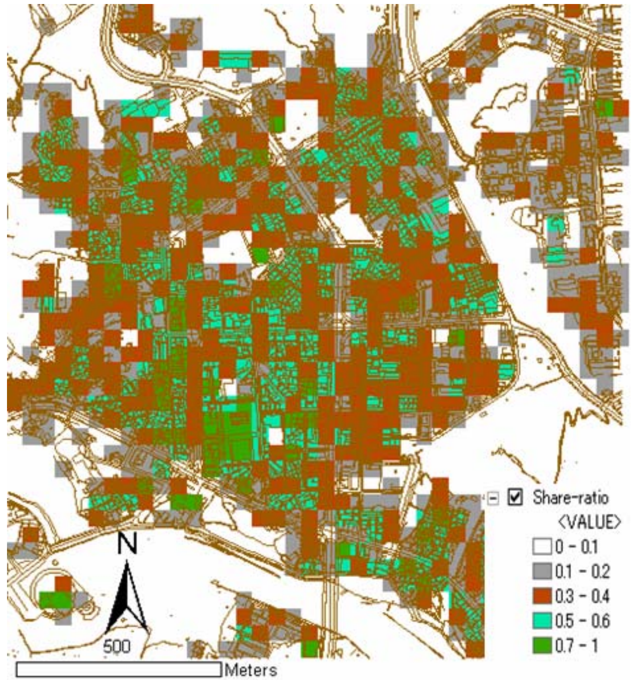

Fig. 3. Share rate of building per unit grid with contour lines.

where u and v are the x- and y-components of flow velocity, respectively; $M^* = \beta M$ and $N^* = \beta N$ are the x- and y-components, respectively, of the corrected discharge per unit width; M and N are the x- and y-components per unit width, respectively; q_{out} is the drainage discharge per unit area from the computational mesh into the sewer system; and q_{over} is the overtopping discharge flow per unit area of the computational grid from the river network. If there are non-linear areas due to the difference of elevation, the discharge flux, M_0 flows by drop-water as:

$$M_0 = \mu h_{\mathrm{h}} \sqrt{g h_{\mathrm{h}}} \tag{14}$$

Based on the hydraulic model test, the discharge coefficient μ is estimated to be $\mu = (2/3)^{3/2}$; and h_{h} is the water depth where the elevation is the highest by over-topping water as (Thang et al., 2004):

$$M_0 = \mu' h_1 \sqrt{g h_1} \tag{15}$$

where μ' is the discharge coefficient estimated as $\mu' = 0.35$; and h_1 is the water depth at the lowest elevation. The minimum depth for moving waters is given as 0.001 m (Iwasa et al., 1980).

4.2 Initial values and model validation

The Samcheok city selected for urban inundation modeling is surrounded by mountains; it mostly consists of low-lying land, where the river flows into the sea through the outside of the city. Following the floods, a field investigation team led

Fig. 4. Inundated depths after flooding.

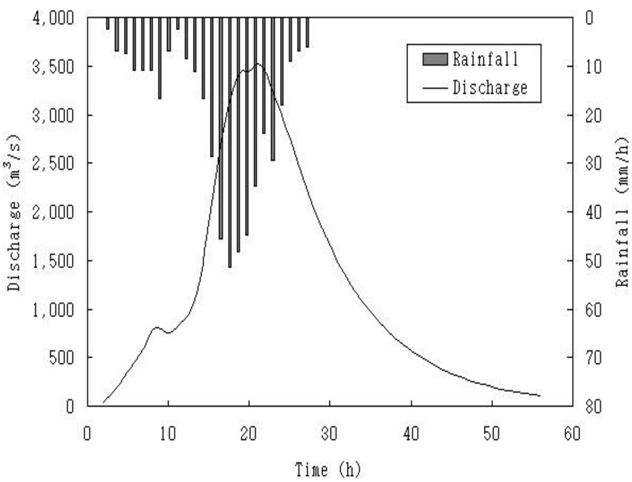

Fig. 5. Discharge hydrograph at bank break point (rainfall data: WAter Management Information System, http://www.wamis.go.kr/).

by city officials was dispatched to the disaster sites in order to gather useful materials (Kang, 2007). Figure 4 shows a sample of a field investigation carried out in the event areas between 31 August and 1 September 2002.

In order to compare the predicted results of the model with the measured data, the model was used to obtain the flood extent and water depth in the urban areas. The information obtained from the field survey was used to create a model comparison between predictions and observations. During this process, a trial-and-error calibration methodology was used in order to determine the Manning's roughness coefficient n, since insufficient flooding data was obtained of Manning's roughness coefficient n in the urban area. There is often a problem when selecting an appropriate DEM size. The DEM size should be selected in such a way that computational time and topographical conditions are acceptable. The computational time step Δt was 0.1 for mountainous areas and 0.2 for urban areas. For the boundary condition in the down stream of the bank break point, the water-level flux of the sides of the grid is assigned using the known discharge hydrograph as shown in Fig. 5.

Table 1. Comparison between computed and observed peak inundation depth in calculation area in case of 2002.

	St. 1	St. 2	St. 3	St. 4	St. 5
Computed (m)	1.16	0.74	0.87	0.89	0.93
Observed (m)	1.35	0.92	0.90	0.80	1.00
dh (m)	−0.19	−0.18	−0.03	0.09	−0.07

dh is difference between computed and observed peak inundation depths in urban area

4.3 Flood flow simulation

The influence of buildings was simulated prior to calculating the urban flow at the time step. The calculated results of urban flooding occurring on 31 August and 1 September 2002, both with and without the inclusion of buildings, are compared as shown in Figs. 6 and 7, respectively. The difference in inundation depth between the two cases of with and without the influence of buildings was significantly greater than had been expected. In the presence of building obstacles, the flow velocity is close to zero, resulting in an increase in the inundation depth. Considering the influence of buildings in the simulation, the inundated water depth increased by about 20–30 cm on most of the modeled area.

The flow of sewer network is quite complicated including the open channel flow and pipe pressure flow. These two kinds of flows are not fixed, they change their state at any moment and form a transient state sometimes. So we applied the open slot method to solve the problem. It is assumed that there is an open slot in the top of the pipe, so that the pipe is equivalent to open channel flow. In order to calculate sewer flow, the cross sectional area of pipe was approximated to rectangular shape for calculating easily and the value of Manning's roughness coefficient is given as $0.015\,\mathrm{s\,m^{-1/3}}$. The flooding water in Samcheok is drained by a pumping station which is designed for a 30-year rainfall. As there was no precise record of the drainage volume from the pumping station during this event, the discharge volume is calculated based on working time. The capacity of the pumping station in the computational area is $2.3\,\mathrm{m^3\,s^{-1}}$. At the first stage of the rainfall event, most of the water can flow into the pipes. This may take place even if the sewer system has sufficient capacity. On the other hand, if the capacity of the pipe system is insufficient, the intake volume is restricted.

The performance of modeling on ArcGIS is shown in Fig. 8. Most of the inundated areas are concentrated in the low elevation region as shown in Fig. 9, while the total

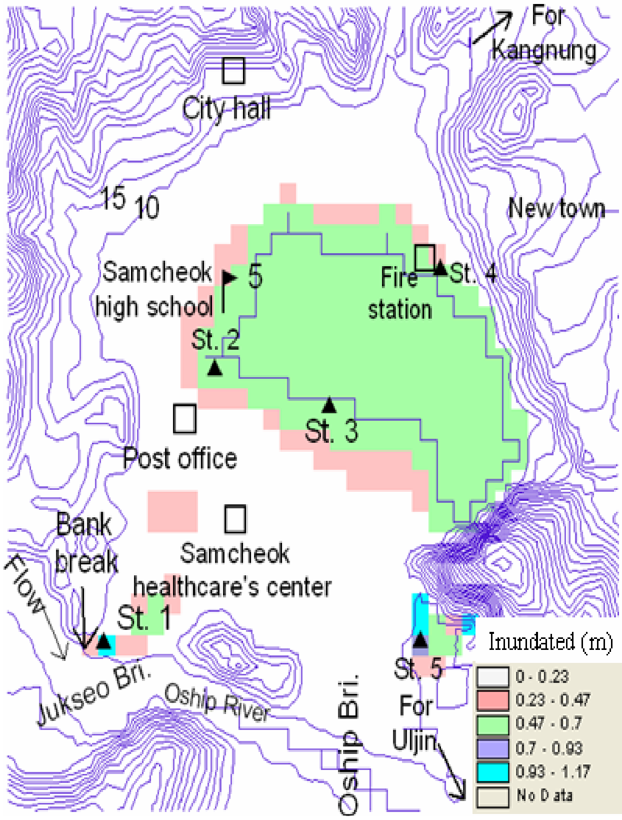

Fig. 6. Inundation depths obtained in the case of no building influence.

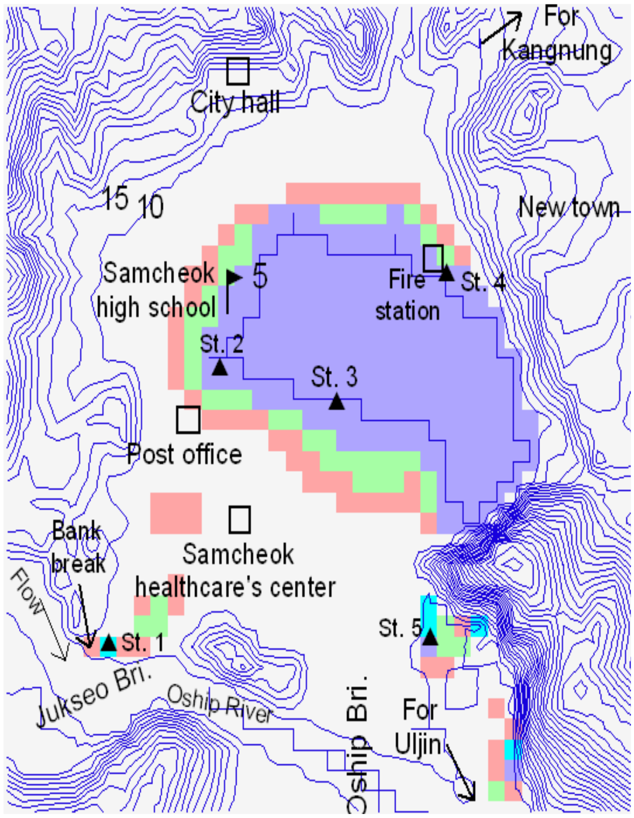

Fig. 7. Inundation depths obtained in the case of building influence.

inundated area is about 0.64 km^2. The results of a comparison between peak water depths at 30 h are given in Table 1. The maximum inundation depths at three locations (St. 3, 4, and 5) appear to be fairly well estimated, while the other two locations (St. 1 and 2) are underestimated with a maximum difference of 19 cm at the maximum inundation time. This underestimation may be due to the topographical uncertainties or street features, where, for example, narrow streets reduce the flow and locally increase the friction. For the estimation of the effects of buildings, the share rate per unit grids is assigned to the computational cells. The share rate of building extracted in most of the computational area was distributed from 0.2 to 0.6. As a result, it is found that the depth and extent of the inundation increased with the influence of buildings. In the case of the urban area, the rainfall on the domain is considered. Where the bank break had not been modeled, the change of flood extent was small, with a decreasing maximum inundation depth of approximately 0.15 m in the low area. Consequently, the effect of rainfall in the urban area will be considerably large and these areas are therefore worth representing. In real events, underground facilities such as large parking areas are critical factors to simulate inundation depth (Nakagawa et al., 2004). However, their effects are neglected in this case since Samcheok does not have large underground facilities.

5 Conclusions

In this paper, an integrated urban flood model of 1-D or 2-D based on GIS was developed to estimate the flooding inundation in dense urban areas. Compared with the traditional separate hydrological models or 1-D and 2-D hydrodynamic models, the proposed model can simulate continuously the inundation state, considering the processes of rainfall-runoff, sewer flow, and urban overland flow. The linking of the GIS platform with hydrodynamic models can greatly improve the estimation of the urban flooding process through the enhanced capabilities to handle large databases that describe the highly complicated characteristics in urban areas.

For simulating urban flood modeling, one of the challenges for the modeler was how best to represent the building resistance. In dense areas, it is likely that buildings will have significant impact on flow routes and inundation. The use of a higher Manning's n value was a common method for representing the energy dissipation caused by building. However, the difficult decision to be made by the modeler is to determine what Manning's n values are appropriate to use.

This study suggests that it may be possible to present the effect of buildings in a 2-D flood modeling by the share rate of buildings instead of by a Manning's higher n value. The method proposed here can consider the resistance factor of

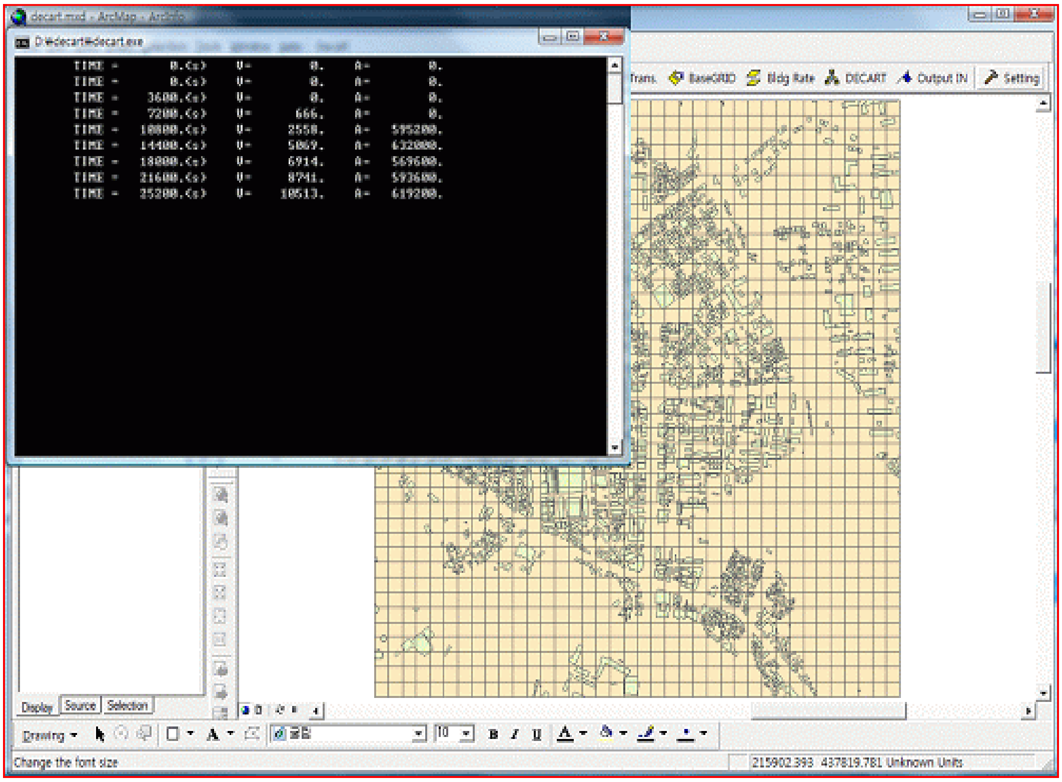

Fig. 8. Calculating inundation depth on ArcGIS.

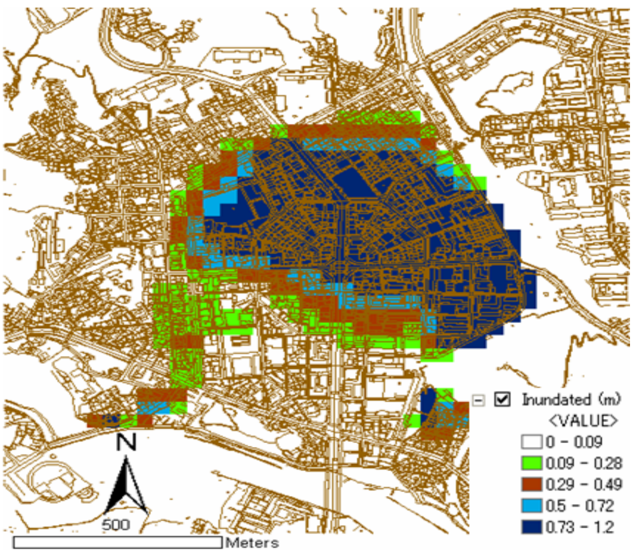

Fig. 9. Simulated results at maximum inundated depth on ArcMap GIS environment.

building varying with its density. It can be concluded that the modeling of urban inundation is feasible on large scale dense areas. The advantage of integrated urban flood modeling by linking GIS is ability to avoid the redundant data exchange of input/output and the contribution to the cost efficient system suffering from urban flooding.

Acknowledgements. The author would like to thank P. Bates and his research group at the University of Bristol, UK, for providing various sample data and reports on their website. The author is also grateful to K. Kawaike at the University of Kyoto, Japan, for providing source code of flood model and useful advices. In addition, part of this research was supported by a grant from the Eco-Star Project (07-||-D) of the Korean Environment Ministry.

Edited by: L. Ferraris
Reviewed by: two anonymous referees

References

Abbott, M. B. and Minns, A. W.: Computational hydraulics, Hampshire, Ashgate press, 1998.

Barrera, A., Llasat, M. C., and Barriendos, M.: Estimation of extreme flash flood evolution in Barcelona County from 1351 to 2005, Nat. Hazards Earth Syst. Sci., 6, 505–518, doi:10.5194/nhess-6-505-2006, 2006.

Bishop, I. D. and Karadaglis, C.: Combining GIS based environmental modeling and visualization: another window on the modeling process, in: Proceedings of Third International Conference/Workshop on Integrating GIS and Environmental Modeling, Santa Fe, NM, USA, 21–25, 1996.

Bourget, P.: Basin-level digital elevation models availability and applications, IWR Report (04-R-1), 2004.

Franz, D. D.: Full equations utilities (FEQUTL) model for the approximation of hydraulic characteristics of open channels and control structures during unsteady flow, Water Resources Investigations Report 97-4037, 1997.

Haile, A. T. and Rientjes, T. H. M.: Effect of LiDAR DEM resolution in flood modelling: a model sensitivity study for the city of Tegucigalpa, Honduras, ISPRS WG III/3, III/4, V/3 Workshop, 168–173, 2005.

Horritt, M. S. and Bates, P. D.: Effects of spatial resolution on a raster based model of flood flow, J. Hydrol., 253, 239–249, 2001a.

Horritt, M. S. and Bates, P. D.: Evaluation of 1D and 2D numerical models for predicting river flood inundation, J. Hydrol., 268, 87–99, 2001b.

Hosoyamada, T.: Numerical analysis of flood around residential area in the Niigata heavy rainfall disaster on 13 July, 2004, Ann. J. Hydraulic Eng., 49, 589–594, 2005.

Iwasa, Y., Inoue, K., and Mizutory, M.: Hydraulic analysis of overland flood flows by means of numerical method, Annuals of DPRI, Kyoto Univ., 23B, 305–317, 1980.

Kang, S. H.: A study on runoff discharge considering economic value of water resource, The Journal of GIS Association of Korea, 15(3), 291–299, 2007.

Kang, S. H.: A framework to estimation GDP loss due to extreme water-related disaster in Kangwon-do, Journal of the Korean Society of Hazard Mitigation, 7(5), 159–166, 2007.

Nakagawa, H., Ishigaki, Y., Muto, Y., Baba, Y., Zhang, H., Yagi, H., and Fujimoto, K.: Experiments and calculations of flood water in urban cities, Annuals of DPRI, Kyoto Univ., 47B, 517–526, 2004.

Nie, L.: Flooding analysis of urban drainage systems, PhD thesis, Norwegian University, 2004.

Sayama, T., Tachikawa, Y., and Takara, K.: Model building unit for rainfall-runoff simulation, Annuals of DPRI, Kyoto Univ., 49B, 27–43, 2006.

Schmitt, T. G., Thomas, M., and Ettrich, N.: Analysis and modeling of flooding in urban drainage systems, J. Hydrol., 299, 300–311, 2004.

Sui, D. Z. and Maggio, R. C.: Integrating GIS with hydrological modeling: practices, problems, and prospects, Computers, Environment and Urban Systems, 23, 33–51, 1999.

Takahashi, K., Nakagawa, H., and Nishizaki, T.: Two dimensional numerical simulation method to estimate the risk of a flood hazard caused by a river bank breach, DPRI, Kyoto Univ., 29B-2, 431–450, 1986.

Takayama, T., Takara, T., Toda, K., Fujita, M., Mase, H., Tachikawa, Y., Yoneyama, N., Tsutsumi, D., and Yasuda, T.: Research Works for the Risk Assessment Technology of Flood in Urban Area and Its Practical Application, Annuals of DPRI, Kyoto Univ., 49C, 39–48, 2006.

Thang, N. K., Inoue, K., Toda, K., and Kawaike, K.: A model for flood inundation analysis in urban area: verification and application, Annuals of DPRI, Kyoto Univ., 47B, 303–316, 2004.

Yang, X. and Rystedt, B.: Predicting Flood Inundation and Risk Using GIS and Hydrodynamic Model: A Case Study at Eskilstuna, Sweden, Indian Cartographer, 183–191, 2002.

Vivoni, E. R.: Richards KT. Integrated use of GIS-based field sampling and modeling for hydrologic and water quality studies, J. Hydroinformatics, 8, 235–250, 2005.